

Nanotherapeutics in angiogenesis: synthesis and in vivo assessment of drug efficacy and biocompatibility in zebrafish embryos

Jinping Cheng^{1*}
Yan-Juan Gu^{2*}
Yajun Wang³
Shuk Han Cheng¹
Wing-Tak Wong²

¹Department of Biology and Chemistry, The City University of Hong Kong, Kowloon, ²Department of Applied Biology and Chemical Technology, The Hong Kong Polytechnic University, Hung Hom, Kowloon, ³Department of Medicine, The University of Hong Kong, Pokfulam, Hong Kong, People's Republic of China

*These authors contributed equally to this work

Background: Carbon nanotubes have shown broad potential in biomedical applications, given their unique mechanical, optical, and chemical properties. In this pilot study, carbon nanotubes have been explored as multimodal drug delivery vectors that facilitate antiangiogenic therapy in zebrafish embryos.

Methods: Three different agents, ie, an antiangiogenic binding site (cyclic arginine-glycine-aspartic acid), an antiangiogenic drug (thalidomide), and a tracking dye (rhodamine), were conjugated onto single-walled carbon nanotubes (SWCNT). The biodistribution, efficacy, and biocompatibility of these triple functionalized SWCNT were tested in mammalian cells and validated in transparent zebrafish embryos.

Results: Accumulation of SWCNT-associated nanoconjugates in blastoderm cells facilitated drug delivery applications. Mammalian cell xenograft assays demonstrated that these antiangiogenic SWCNT nanoconjugates specifically inhibited ectopic angiogenesis in the engrafted zebrafish embryos.

Conclusion: This study highlights the potential of using SWCNT for generating efficient nanotherapeutics.

Keywords: carbon nanotubes, drug delivery, antiangiogenic therapy

Introduction

Tumor angiogenesis is an essential step in tumor progression and metastasis formation, and also provides important targets for tumor diagnosis and therapy. Antiangiogenic strategies have been pursued for cancer treatment and prevention of cancer recurrence and metastasis.^{1,2} A variety of antiangiogenic agents, which lead to inhibition of angiogenesis, such as platelet factor 4, angiostatin, endostatin, and vasostatin, are already in the clinical trials.³ However, antiangiogenic therapies usually have toxic side effects without specific targeting. Molecules associated with angiogenesis are now being considered as attractive targets for inhibition of angiogenesis. Recent evidence indicates that vascular integrins, in particular alpha-v-beta-3 ($\alpha_v\beta_3$), are important regulators of angiogenesis, including tumor angiogenesis. Integrin $\alpha_v\beta_3$ is highly expressed on activated endothelial and tumor cells, but is not present in resting endothelial cells and most normal organ systems. This property makes it a suitable target for antiangiogenic cancer therapy.² The cyclic arginine-glycine-aspartic (RGD) peptide recognizes $\alpha_v\beta_3$ integrin receptors and has been widely used for detection of $\alpha_v\beta_3$ expression.^{4,5}

Carbon nanotubes are a potential and promising vector for drug delivery, with a relatively long blood circulation time and intrinsic transporting ability.⁶ Carbon

Correspondence: Wing-Tak Wong
Department of Applied Biology and
Chemical Technology, The Hong Kong
Polytechnic University, Hung Hom,
Kowloon, Hong Kong, China
Tel +852 3400 8789
Fax +852 2364 9932
Email bcwtwong@polyu.edu.hk

nanotube-biomolecule nanoconjugates have been used in proof-of-principle experiments to demonstrate targeting to desired cell populations for immune recognition or to achieve therapeutic effects.^{7,8} In a pilot study that assessed the interactions of carbon nanotubes in zebrafish embryos, we found that carbon nanotubes are distributed in the blastoderm cells, but not in the yolk.⁹ This property facilitates effective drug delivery in zebrafish because most of the important events occur in the blastoderm cells. Furthermore, carbon nanotubes can be distributed by blood flow throughout the whole cardiovascular system in transparent zebrafish embryos.⁹

Embryonic circulation and development of blood vessels have been studied in detail in the zebrafish.¹⁰ Zebrafish embryos are transparent, which facilitates visual inspection of the cardiovascular system as well as changes in blood vessel growth. At 24 hours following fertilization, the major vessels, aorta (dorsal artery), and posterior cardinal vein are formed. These major vessels are formed by the process of vasculogenesis.¹¹ The whole vasculature is established by 72 hours following fertilization.¹² Furthermore, the formation of zebrafish blood vessels by angiogenic sprouting appears to require the same proteins shown to be necessary for blood vessel growth in mammals.¹³ The pattern of blood vessel development is almost the same between individual embryos.¹⁴

In zebrafish embryos, subintestinal vessels originate from the duct of the Cuvier at 48 hours following fertilization, and these vessels supply the digestive system. At 24–48 hours following fertilization, the subintestinal vessels form a vascular plexus by angiogenesis across most of the dorsal-lateral aspect of the yolk ball,¹⁰ and the plexus is apparent by 72 hours following fertilization.¹⁵ Because the vascular plexus of the subintestinal vessels can be seen, it has been widely used as a structural parameter for determination of either pharmacological angiogenesis or inhibition of the angiogenesis process. Defects in the development of the zebrafish embryo vascular system can be visualized and recorded by live imaging analysis using either microangiography or transgenic zebrafish embryos.

In the present study, we used transparent zebrafish embryos and functionalized carbon nanotubes to study nanotherapeutics in angiogenesis. Single-walled carbon nanotubes (SWCNT) were conjugated with three different agents for multimodal drug delivery. The conjugated agents included the antiangiogenesis drug, thalidomide, a peptide cyclic RGD for angiogenesis-specific targeting, and a fluorescent marker at noncompeting binding sites. Thalidomide was chosen as an antiangiogenesis therapeutic agent because it is a widely used

anticancer drug for the treatment of many cancers.^{16,17} Cyclic RGD peptides recognize angiogenesis, and are a marker for the identification of angiogenesis in many cancer models.^{4,5} The fluorescent marker, rhodamine (Rh), allows the tracking of SWCNT inside mammalian cells and zebrafish embryos under confocal microscopy. The biodistribution and ectopic angiogenesis-targeting efficacy of triple-coated SWCNT were investigated in zebrafish embryos. The targeted antiangiogenesis therapy was then studied in a zebrafish tumor xenograft angiogenesis assay.

Materials and methods

Thalidomide analogs and SWCNT conjugates

SWCNT were purchased from Nanostructured and Amorphous Materials Inc (Houston, TX). Thalidomide, polyoxyethylene bis(amine) (NH₂-PEG-NH₂, with an molecular weight of 3350), N-hydroxy succinimide (NHS) and N-(3-dimethylaminopropyl)-3-ethylcarbodiimide hydrochloride (EDC) were purchased from Sigma-Aldrich (St Louis, MO). 2-(Boc-amino) ethyl bromide was purchased from Fluka. NHS-Rh, succinimidyl 4-(N-maleimidomethyl) cyclohexane-1-carboxylate (SMCC), and N-succinimidyl S-acetylthioacetate (SATA) were purchased from Pierce (Rockford, IL). Unless specified, the chemicals and reagents were used as received from the relevant commercial sources. A Microcon centrifugal filter device (YM-100, regenerated cellulose 10,000 molecular weight cutoff) was purchased from Millipore (Billerica, MA). A Spectra/Por[®] dialysis membrane (molecular weight 12,000–14,000) was purchased from Spectralabs (Rancho Dominguez, CA).

Thalidomide was first modified with 2-(Boc-amino) ethyl bromide to generate the amino group, and then the compound was conjugated with SATA to yield the thiolated thalidomide (denoted as thalidomide-SH). The experimental details for the synthesis of thalidomide analogs can be found in the Supplementary Materials section.

The raw SWCNT were first oxidized to obtain oxidized SWCNT, and then the oxidized SWCNT were conjugated with polyethylene glycol (PEG) to yield PEGylated SWCNT. The PEGylated SWCNT were labeled with NHS-Rh and fluorescein isothiocyanate (FITC) to generate Rh-labeled SWCNT (Rh-SWCNT) and FITC-SWCNT, respectively. The RGD-SH was synthesized by Dr Cong Li from the School of Pharmacy at Fudan University (Shanghai, China). The FITC-SWCNT were first reacted with SMCC to produce FITC-SWCNT-SMCC, and then further reacted with RGD-SH in the presence of 10 mM Tris(2-carboxyethyl)

phosphine hydrochloride (TCEP) at pH 7.4 to yield FITC-SWCNT-RGD. Rh-SWCNT was also firstly reacted with SMCC to produce Rh-SWCNT-SMCC, and Rh-SWCNT-SMCC conjugates were reacted overnight with RGD-SH and thalidomide-SH in the presence of 10 mM TCEP at pH 7.4 to obtain RGD-SWCNT(Rh)-thalidomide and Rh-SWCNT-RGD conjugates. The molar ratio of RGD-SH to thalidomide-SH is 1:5. Because the effective concentration of thalidomide is higher than that of RGD, a combination of a high ratio of thalidomide and low ratio of RGD was adopted in the study. The concentration of thalidomide loaded onto the SWCNT was measured by the absorbance peak at 299 nm (characteristic of thalidomide). The detailed synthesis procedures and characterization measurement information of all SWCNT-based conjugates can be found in the Supplementary Materials section. All SWCNT-based conjugates were dissolved in 1× phosphate-buffered saline for related biological experiments.

¹H nuclear magnetic resonance (NMR) spectra were measured on a Varian 300 or Varian 400-MR spectrometer (Agilent Technologies, Inc, Santa Clara, CA). Electrospray ionization (ESI) mass spectroscopic (MS) data were determined with a ThermoFinnigan LCQ™ (Thermo Scientific, Waltham, MA) electrospray ionization mass spectrometer. Ultraviolet-visible spectra were recorded on a Thermo Spectronic UV1 spectrometer. The morphologies and structures of SWCNT and RGD-SWCNT(Rh)-thalidomide conjugates were characterized by transmission electron microscopy (TEM, Tecnai 20; Philips, Amsterdam, the Netherlands) with an accelerating voltage of 200 kV. The samples were prepared by drying droplets of a sample in ethanol dispersed onto carbon-coated copper grids. The purity of PEG-modified SWCNT was estimated by thermogravimetric analysis, which was performed on a Pyris-1 (Perkin Elmer, Waltham, MA) sphere thermal analysis system under flowing air at a scan rate of 20°C/minute from 50°C to 800°C.

Human cell culture experiments

The four mammalian cancer cell lines used in this study were obtained from the American Type Culture Collection (ATCC, Manassas, VA), namely, human glioblastoma cancer cells U87MG (ATCC HTB-14), human breast cancer cells MCF-7 (ATCC HTB-22), ovarian SKOV3 carcinoma cells (ATCC HTB-77), and human HT1080 fibrosarcoma cells (ATCC CCL-121). Integrin $\alpha_v\beta_3$ -positive cells (U87MG) and integrin $\alpha_v\beta_3$ -negative cells (MCF7) were used to study the targeting efficacy of RGD-labeled SWCNT. Ovarian SKOV3 carcinoma cells which carried a plasmid-expressing enhanced

green fluorescent protein (pEGFP; SKOV3:pEGFP) was used to establish the zebrafish xenograft assay. Human HT1080 fibrosarcoma cells, the proangiogenic mammalian tumor cells, were used for induction of ectopic angiogenesis in the zebrafish cancer model. The cells were cultured in Dulbecco's modified Eagle's medium (Invitrogen, San Diego, CA). The media were supplemented with 10% fetal bovine serum (Invitrogen), 100 U penicillin, and 10 µg/mL streptomycin (Invitrogen) in 5% CO₂, in 95% air at 37°C in a humidified incubator. After incubating the cells with FITC-SWCNT or FITC-SWCNT-RGD at 37°C (CO₂ 5%) for 3–4 hours, the cells were rinsed with fresh culture medium and imaged by a Leica confocal laser scanning microscope (SPE or SP5; Leica Camera AG, Solms, Germany) combination system equipped with a Plan-Neofluar 40 × 1.3 NA oil DIC objective.

Maintenance of zebrafish

Friend leukemia integration 1a (*fli1a*) is a transcription factor constitutively expressed in endothelial cells. Transgenic *fli1a:EGFP* zebrafish containing fluorescently labeled endothelial cells were used to study the experimental antiangiogenic therapy in vivo. Generation and characterization of the *fli1a:EGFP* lines has been described in detail in the literature.¹⁸ In transgenic zebrafish, the promoter of the endothelial marker, *fli1a*, drives the expression of EGFP in the blood vessels. The formation of the embryonic vasculature can be visualized in the transgenic *fli1a:EGFP* zebrafish as well.

Wild-type mature zebrafish (*Danio rerio*) were purchased from a local commercial source (Chong Hing Aquarium, Hong Kong, China). The transgenic *fli1a:EGFP* zebrafish were purchased from Zebrafish International Resource Center (Eugene, OR). The zebrafish colony was maintained as previously described.¹⁹ Adult zebrafish were maintained in charcoal-filtered tap water supplemented with salts and kept in 14-hour light: 10-hour dark cycles. The embryos were obtained by photoinduced spawning over green plants and cultured at 28.5°C in filtered tap water. The developmental stage of the embryos was measured according to the number of hours following fertilization and staged according to a method described elsewhere.²⁰

Injection of SWCNT into zebrafish embryos to study biodistribution

The fluorescent Rh-SWCNT and Rh-SWCNT-RGD were loaded into the cell of wild-type zebrafish embryos by microinjection at the one-cell stage to study in vivo biodistribution. After the light was turned on for photoinduced spawning, the embryos were collected within 15 minutes after fertilization

and selected under a dissecting microscope for microinjection for the one-cell stage experiments. Zebrafish embryos were collected into a microinjection plate filled with incubation medium. The Rh-SWCNT or Rh-SWCNT-RGD was then injected into the embryonic cell or yolk of the embryos with a nitrogen-driven microinjector (Narishige) within 45 minutes of fertilization. After microinjection, the embryos were incubated at 28.5°C for further development and imaged on a Olympus Disk Scanning Unit (DSU, Olympus, Tokyo, Japan) using internal DSU filter CY3 cubes at critical time points. Wild-type zebrafish embryos from the same clutch that were not injected were used as controls. All embryos were cultured in embryo medium which contained 0.2 mM 1-phenyl-2-thiourea (PTU) from 24 hours following fertilization to inhibit pigment development.

Zebrafish wound healing model

The fluorescent dye-labeled Rh-SWCNT-RGD was loaded into the yolk of transgenic *fli1a:EGFP* zebrafish embryos by microinjection at the one-cell stage as described above. Transgenic zebrafish embryos from the same clutch that were not injected were used as controls. To study angiogenesis targeting through the use of RGD-SWCNT nanoconjugates, a zebrafish wound healing model was adopted for this study. At 48 hours following fertilization, 20 embryos were anesthetized with 0.016% (w/v) tricaine (ethyl 3-aminobenzoate methanesulfonate, Sigma-Aldrich). The wound site was then generated on the trunk area of the embryos using the tip of a pair of forceps, without destruction of the circulatory system. At 72 hours following fertilization, the embryos were assessed under DSU using internal DSU filters GFP and CY3 cubes.

Antiangiogenic activity of thalidomide-SWCNT conjugates

Transgenic *fli1a:EGFP* zebrafish embryos were used to study the antiangiogenic activity of thalidomide and its conjugates. Thalidomide was dissolved in dimethyl sulfoxide to make up a 400 mM stock solution. To make the stock solution, thalidomide in dimethyl sulfoxide was heated for 2 minutes at 65°C and shaken vigorously for 2 minutes at room temperature, and repeated more than ten times. A higher concentration of thalidomide stock was required to keep the final concentration of dimethyl sulfoxide under 0.1% in the exposure experiments. The thiolated thalidomide and thalidomide-SWCNT were dissolved in water. Twenty transgenic *fli1a:EGFP* zebrafish embryos at 4 hours following fertilization were placed into 2.5 mL of dosing solution that contained 0.2 mM PTU and

allowed to develop at 28.5°C. The treated embryos were assessed at 48 hours following fertilization under a confocal microscope. The embryos were anesthetized in 0.016% (w/v) tricaine prior to observations.

Xenograft angiogenesis assay in zebrafish embryos

The method of xenograft angiogenesis assay in zebrafish embryos was used to study the therapeutic effect of synthesized nanotherapeutics. Both wild-type and transgenic *fli1a:EGFP* zebrafish were used in the xenograft angiogenesis assay. Wild-type zebrafish embryos were xenografted with ovarian SKOV3 carcinoma cells which carried a pEGFP (SKOV3:pEGFP) with nanoconjugates to establish the assay. Transgenic *fli1a:EGFP* zebrafish embryos were xenografted with human fibrosarcoma cells HT1080 with or without nanoconjugates to study the therapeutic effects.

Existing procedures for xenograft angiogenesis assay in zebrafish embryos were adopted²¹ with some modifications. At 4 hours following fertilization, the embryos were examined under a dissecting microscope, and only embryos that developed normally and reached the blastula stage were selected for subsequent experiments. All selected embryos were cultured in embryo medium that contained 0.2 mM PTU, starting from 24 hours following fertilization. At 48 hours following fertilization, the zebrafish embryos were dechorionated and then anesthetized using 0.016% (w/v) tricaine. The anesthetized zebrafish embryos were laterally mounted in a 0.3% agarose-coated Petri dish covered with embryo culture medium, and the embryos were orientated with the yolk on a flank. The orientated embryos were injected with 1000–2000 mammalian cancer cells per embryo and resuspended in 3–4 nL of Matrigel (Becton Dickinson, Franklin Lakes, NJ) using a Picospritzer microinjector (Eppendorf, Hamburg, Germany). The pipette was calibrated every time before microinjection. The calibration of the microinjection pipette was performed by injecting the solution into mineral oil and quantifying the volume. Injection of the same volume of Matrigel solution was used as the negative control. The detailed protocol for cell injection has been described in the literature.²¹ In each experiment, a total of 15 embryos were injected with Matrigel only, HT1080 cells only, and both HT1080 cells and RGD-SWCNT(Rh)-thalidomide (1.2 mg/mL of SWCNT, with 0.334 mg/mg thalidomide and 0.125 mg/mg RGD on SWCNT), respectively. The experiments were repeated separately four times.

After injection, the embryos were incubated in embryo medium containing 0.2 mM PTU for another 24 hours

before imaging. The embryos were imaged live at 72 hours following fertilization by a Leica confocal laser scanning microscope (SPE or SP5) combination system equipped with a Plan-Neofluar 40×1.3 NA oil DIC objective. The images were then further processed for scoring of vascular changes and quantification analysis of subintestinal vessel formation. The embryos were anesthetized in 0.016% (w/v) tricaine prior to observation.

Vascular changes and subintestinal vessel formation

The subintestinal vessels form on the dorsolateral surface of the yolk on both sides of the embryo in the shape of a basket over the yolk.¹² In this study, proangiogenic or antiangiogenic effects are defined as either a gain or loss of either the lateral or ventral vessel of the basket. In order to compare the effects of different treatments on angiogenesis, we quantified vessel formation. The subintestinal vessels in the transgenic *flil1a:EGFP* zebrafish were visualized under confocal microscopy. A quantitative analysis was performed on a PC computer using the public domain NIH Image program (developed at the US National Institutes of Health and publicly available on the Internet at <http://rsb.info.nih.gov/nih-image/>). Using this software, the overall length of the subintestinal vessels was quantified by manual point to point measurement, and the area of the subintestinal vessels was quantified in a similar way.

Results

Synthesis and characterization of RGD-SWCNT(Rh)-thalidomide nanoconjugates

To evaluate the targeting and efficacy of the SWCNT-based drug delivery system, we designed and synthesized fluorescently-labeled SWCNT conjugates. The fluorescent dye-labeled SWCNT, FITC-SWCNT, and FITC-SWCNT-RGD were used to track the internalization of PEGylated SWCNT and SWCNT-RGD, respectively, in the tumor cells. Fluorescence Rh-labeled SWCNT conjugates, Rh-SWCNT, Rh-SWCNT-RGD, and RGD-SWCNT(Rh)-thalidomide were designed as fluorescent molecular probes for the SWCNT-based conjugates for tracking the biodistribution of SWCNT and drug release in zebrafish embryos.

To couple thalidomide with SWCNT, thalidomide 1 was initially coupled with 2-(Boc-amino) ethyl bromide in the presence of sodium hydride and dimethylformamide (DMF) to form thalidomide 2 (Figure S1, Supplementary materials). A free sulfhydryl group was then grafted to thalidomide 2

through modification with the heterobifunctional linker, SATA, followed by reaction with hydroxylamine. The thalidomide derivatives were structurally characterized by ultraviolet-visible spectroscopy, ¹H nuclear magnetic resonance (NMR) and ESI-MS (detailed in the Supplementary materials section).

The synthesis of SWCNT-based conjugates is illustrated in Figure 1 and the Supplementary Materials section. Raw SWCNT were first functionalized and purified by oxidation in concentrated HNO₃ to obtain SWCNT 2. The ends and defect sites on the side wall of the oxidized SWCNT were functionalized with carboxylic acid and carboxylate groups, which have been summarized in a previous review.²² These carboxylic acid and carboxylate groups were subsequently reacted with amine moieties through carbodiimide-activated coupling with diamine-terminated PEG (PEG_{3500N}) to give PEGylated SWCNT 3. The TEM image of raw SWCNT is shown in Figure 2A. The average diameter of SWCNT is about 1–2 nm. The length of the SWCNT in the raw sample was 5–30 μm. However, the majority of the SWCNT were found to be 100–800 nm in length, with a mean length of 200 nm after oxidation and modification, as statistically estimated by TEM images. In addition, the purity of PEG-modified SWCNT was characterized by thermogravimetric analysis. Figure 2B shows the thermogravimetric analysis curves from H₂N-PEG-NH₂, raw SWCNT, and SWCNT-PEG-NH₂. Upon heating in air, all species that were present in the SWCNT were converted to their corresponding oxides. The H₂N-PEG-NH₂ started to decompose at 200°C, and 95% of the H₂N-PEG-NH₂ was decomposed at 400°C (dashed line). It is also seen that the mass of raw SWCNT quickly decreased at 500°C (dotted line). There was still 15.9% of the residual weight after thermal decomposition. In contrast, the thermogravimetric analysis measurement of SWCNT-PEG-NH₂ (solid line) showed two main large bands in the weight percent decrease curve. Assuming that the mass loss occurring during the first thermal decomposition of the SWCNT-PEG-NH₂ sample was due entirely to the removal of the H₂N-PEG-NH₂, the residual weight after the first decomposition (80%) implies a SWCNT content as high as 20%. The residual weight after the second decomposition is about 0.07%, which indicates high purity of SWCNT after oxidation and modification.

The amount of reactive amine group on PEG-modified SWCNT was estimated to be 2.8×10^{-6} mol/mg, which was measured by quantifying pyridine-2-thion following reaction with N-succinimidyl 3-(2-pyridylthio) propionate (SPDP).^{23,24} The fluorescent Rh molecule was reacted with

In vitro angiogenesis inhibition using FITC-SWCNT-RGD

In order to study the penetration properties of PEGylated SWCNT, we also synthesized FITC-labeled SWCNT conjugates, including FITC-SWCNT and FITC-SWCNT-RGD (Figure S2, Supplementary Materials). The integrin $\alpha_v\beta_3$ -positive cells (U87MG) and integrin $\alpha_v\beta_3$ -negative cells (MCF7) were incubated with FITC-SWCNT (0.12 mg/mL of SWCNT, and 0.45×10^{-7} mol/mg of FITC on SWCNT), respectively. After 4 hours of coincubation, the fluorescence of exposed live cells was detected by confocal microscopy. It was found that a much higher fluorescent signal is observed in MCF7 cells, whereas little fluorescence is observed in U87MG cells. Since the cytomembrane is impermeable to FITC,⁷ the high fluorescence signals in Figure 3A correspond to the FITC labeled on the SWCNT taken up by MCF7 cells. The fluorescence intensity was measured and analyzed using MetaMorph (Universal Imaging, Downingtown, PA). The relative fluorescent intensity from the intracellular FITC-SWCNT in the MCF7 cells (Figure 3A) was 3.4 times stronger than that in the U87MG cells (Figure 3D). This result indicates that, at the same dose and exposure conditions, FITC-SWCNT have a higher affinity for MCF7 cells than for U87MG cells.

We then studied the targeting efficiency of FITC-SWCNT-RGD to U87MG and MCF-7 cells further. After

incubation with FITC-SWCNT-RGD (0.12 mg/mL of SWCNT, 12.5 μ g/mg RGD, and 0.45×10^{-7} mol/mg of FITC on SWCNT) for 3 hours, the U87MG cells began to show a growth inhibition effect while MCF7 was little affected, as indicated by their morphological changes shown in Figure 3C and F. Furthermore, a much higher fluorescence signal was observed in the U87MG cells and little fluorescence signal was observed in the MCF7 cells. The relative fluorescent intensity from the intracellular FITC-SWCNT-RGD in the MCF7 cells (Figure 3B) is only 58% of that in the U87MG cells (Figure 3E). Due to the low integrin $\alpha_v\beta_3$ expression in the MCF7 cells, very low levels of FITC-SWCNT-RGD in the MCF7 cells was observed. With a high integrin $\alpha_v\beta_3$ expression in the U87MG cells, FITC-SWCNT-RGD can selectively recognize U87MG cells with RGD, and afford little destruction of integrin $\alpha_v\beta_3$ -negative cancer and normal cells. Considering the high affinity of SWCNT-FITC to MCF7 cells, these results show that FITC-SWCNT-RGD affords efficient angiogenesis targeting in vitro.

Biodistribution of Rh-SWCNT-RGD in zebrafish embryos

Zebrafish embryos loaded with PEGylated SWCNT at the one-cell stage developed normally to the larval stage (data not shown), in which embryos loaded with multiwalled carbon nanotubes showed a similar effect.⁹ After being introduced

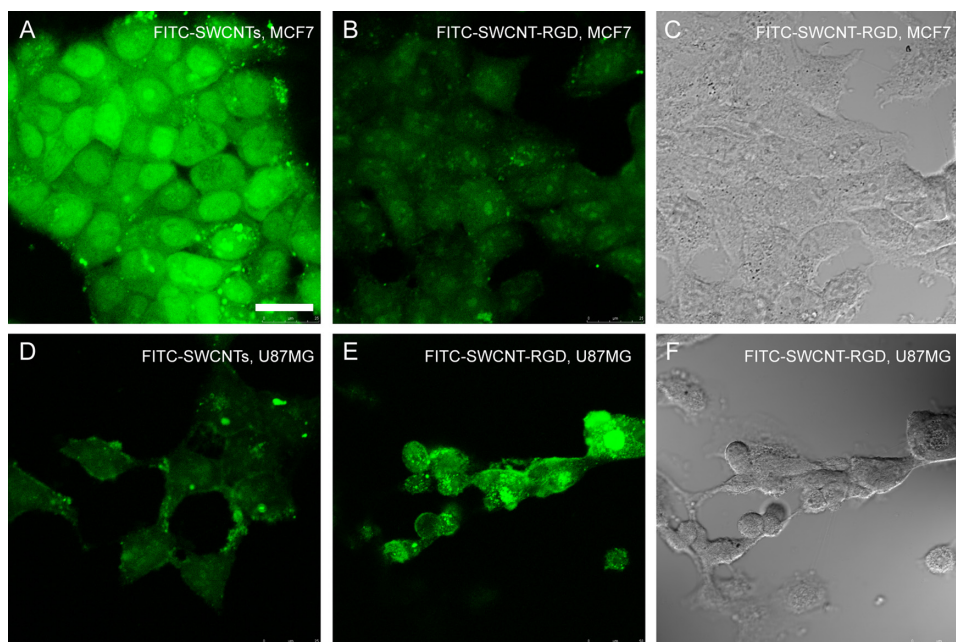


Figure 3 Confocal microscopic images of MCF7 cells (A, B and C) and U87MG cells (D, E and F) incubated with FITC-SWCNT (A and D) and FITC-SWCNT-RGD (B, C, E and F). (A) and (F) are the bright view images of (B) and (E), respectively. The green fluorescent signals indicate the location of FITC-SWCNT (A and D) and FITC-SWCNT-RGD (B and E) in the cells. Scale bar: 25 μ m.

Abbreviations: RGD, cyclic arginine-glycine-aspartic peptide; SWCNT, single-walled carbon nanotubes; FITC, fluorescein isothiocyanate.

into embryonic cells at the one-cell stage, the Rh-SWCNT were allocated to all the blastoderm cells but not the yolk through cell division (data not shown). In order to determine whether the conjugation of RGD affects biodistribution, Rh-SWCNT-RGD were introduced into zebrafish embryos at the one-cell stage by microinjection. About 2.4 ng of SWCNT and 0.3 ng of RGD were loaded into the injected embryos, with an injection volume of about 2 nL. The biodistribution profiles of Rh-SWCNT-RGD were time lapse-imaged by DSU microscopy at several important time points in live zebrafish embryos, and the representative images are shown in Figure 4. It was found that Rh-SWCNT-RGD displays a similar biodistribution pattern as Rh-SWCNT, with a dominant blastoderm cell distribution. Loaded Rh-SWCNT-RGD were excluded from the yolk, even though there were frequent exchanges between the blastoderm cells and the yolk during embryonic development. The dominant blastoderm cell distribution of Rh-SWCNT-RGD implies effective drug delivery in zebrafish given that most of the important events occur in the blastoderm cells.

Angiogenesis targeting by RGD-SWCNT nanoconjugates

In this study, a wound healing-associated angiogenesis model was used to study the angiogenesis-targeting ability of Rh-SWCNT-RGD. Angiogenesis, the growth of new blood

vessels, is an important natural process required for wound healing and restoring blood flow to tissues after an injury or insult. Immediately following an injury, angiogenesis is initiated by multiple molecular signals.²⁵ During angiogenesis, both structural and inflammatory cells in different tissues are involved in the mechanisms of endothelial cell proliferation, migration, and activation, through the production and release of angiogenic mediators.²⁶

The zebrafish wound site was generated at 24 hours following fertilization, but the recovery process was so fast during early development that the embryos were able to recover totally from the wound without leaving any scars for identification (data not shown). When the wound site was generated at 48 hours following fertilization, 20 treated embryos all showed a scar structure on the trunk at 72 hours following fertilization. As shown in Figure 5A, the wound site is marked in the red boxed area, and the FITC channel (Figure 5C) clearly shows angiogenesis in the wound site. In the Rh channel (Figure 5B), an accumulated yellow signal is observed in the wound site, which indicates specific targeting of Rh-labeled RGD-SWCNT. Because integrin $\alpha_v\beta_3$ is also overexpressed on the activated endothelial cells during wound healing,²⁷ the effective integrin $\alpha_v\beta_3$ -targeting ability of RGD serves as a valuable marker of angiogenesis after ischemic injury, myocardial infarction, and inflammation. In this study, RGD-SWCNT conjugates preserved the specific angiogenesis-targeting ability after 72 hours of loading inside the zebrafish, which indicates that the nanoconjugates help to prevent degradation of cyclic RGD peptide and preserves its activity in vivo. After being distributed inside the embryos for 72 hours, the RGD-SWCNT conjugates can still move towards the targeted site and thus allow detection of the distinct proangiogenesis signal generated from the wound healing process which is different from other sites with a novel level of angiogenesis. In contrast with loading into the embryonic cell at the one-cell stage, a certain amount of the loaded SWCNT remains inside the yolk part, although quite a large portion of the loaded SWCNT is allocated to the blastoderm cells, as indicated by the yellow signal in Figure 5B. Another two of the untreated *fli1a:EGFP* zebrafish larvae show a normal morphology of the trunk part without any wounds, and the GFP fluorescent channel demonstrates the blood vessel system in normal embryos.

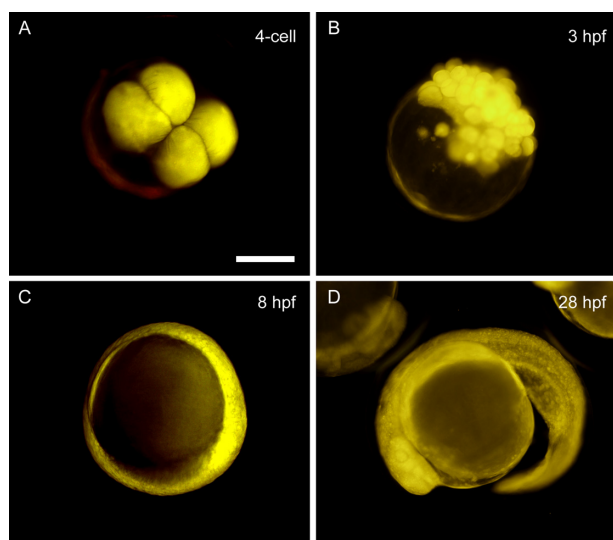


Figure 4 In vivo biodistribution of Rh-SWCNT-RGD in developing zebrafish embryos at different developmental stages. Zebrafish embryos were loaded with 2 nL of Rh-SWCNT-RGD (2.4 ng of SWCNT and 0.3 ng of RGD) into embryonic cells at the one-cell stage through microinjection. According to the red fluorescence signal from Rh-SWCNT-RGD, the loaded Rh-SWCNT-RGD are distributed into the blastoderm cells, but not the yolk cells, at all observed developmental stages, including the four-cell stage (A), 3 hours following fertilization (B), 8 hours following fertilization (C), and 28 hours following fertilization (D). Scale bar: 200 μ m.

Abbreviations: RGD, cyclic arginine-glycine-aspartic peptide; SWCNT, single-walled carbon nanotubes; Rh, rhodamine.

Angiogenesis inhibition by thalidomide-SWCNT nanoconjugates

Thalidomide-induced antiangiogenic activity was confirmed in the zebrafish embryos. The lowest effective concentration of thalidomide in the zebrafish embryos was 2 mg/mL. After

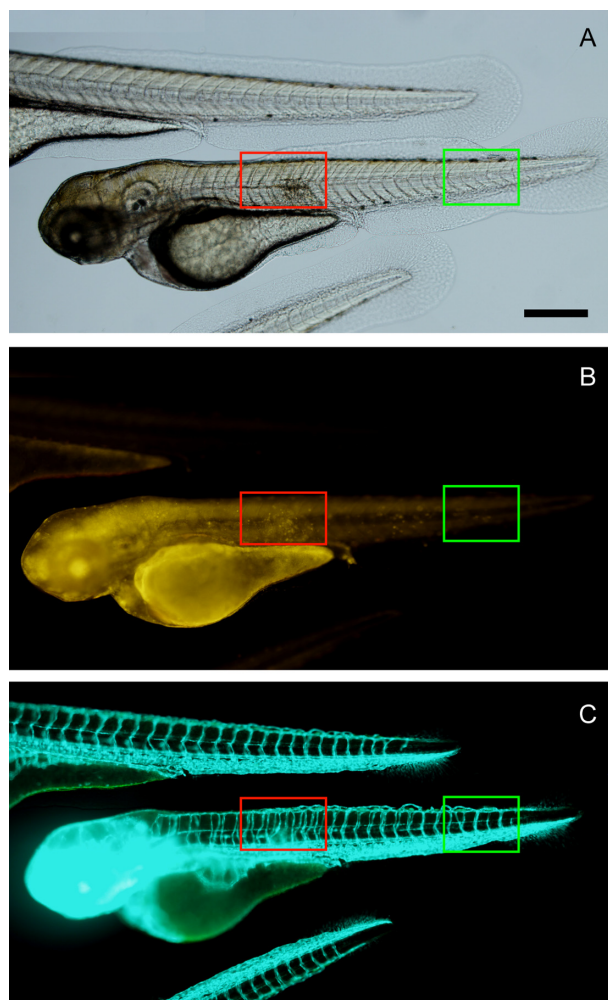


Figure 5 In vivo angiogenesis targeting of Rh-SWCNT-RGD in zebrafish wound healing model. By imaging transgenic *fli1a:EGFP* zebrafish that contained fluorescently-labeled endothelial cells, angiogenesis associated with wound healing in transgenic zebrafish embryos can be observed by checking the GFP signal. (A) Bright view and (B) Rh channel. Red fluorescence indicates the location of Rh-SWCNT-RGD in the zebrafish embryos. (C) indicates the FITC channel. Green fluorescence indicates distribution of fluorescently-labeled endothelial cells in transgenic zebrafish embryos. The red boxed area marks the region with a wound. The green boxed area marks a normal region in the zebrafish trunk. Scale bar: 150 μ m.

Abbreviations: RGD, cyclic arginine-glycine-aspartic peptide; SWCNT, single-walled carbon nanotubes; Rh, rhodamine; FITC, fluorescein isothiocyanate; EGFP, enhanced green fluorescent protein.

modification, thiolated thalidomide demonstrated antiangiogenic activity at a relatively lower concentration, and the lowest effective concentration of thiolated thalidomide was about 0.4 mg/mL. To determine whether thalidomide-SWCNT have similar effects on the zebrafish embryos, the zebrafish embryos were treated with 0.334 mg/mg thalidomide-SWCNT (SWCNT concentration 1.2 mg/mL). The effects of thalidomide on angiogenic vessel formation was assessed using transgenic *fli1a:EGFP* zebrafish embryos. Blood vessel patterning is highly characteristic in developing zebrafish embryos, and intersegmental blood vessels can be easily visualized microscopically by imaging transgenic

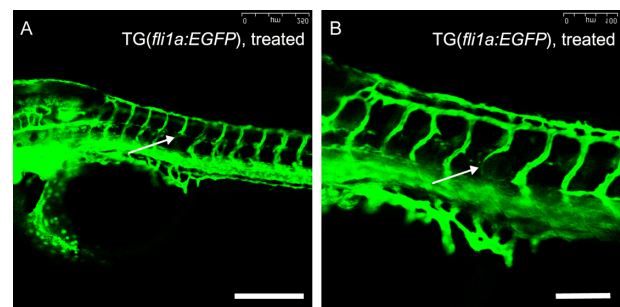


Figure 6 Inhibitory effects of SWCNT-conjugated thalidomide on angiogenesis in transgenic zebrafish embryos. Transgenic *fli1a:EGFP* zebrafish embryos were treated with 0.334 mg/mg thalidomide-SWCNT (thalidomide concentration, 1.2 mg/mL of SWCNT) from 4 hours following fertilization to 48 hours following fertilization, and then visualized live under a Leica SPE confocal microscope. The absence (A) and thinning (B) of intersegmental blood vessels, as indicated by the white arrows, is randomly distributed in zebrafish embryos after treatment with SWCNT-thalidomide. Scale bar: 250 μ m in (A) and 100 μ m in (B).

Abbreviation: SWCNT, single-walled carbon nanotubes.

fli1a:EGFP zebrafish that contain fluorescently-labeled endothelial cells. Treatment with 0.334 mg/mg thalidomide-SWCNT (1.2 mg/mL of SWCNT) for 44 hours showed inhibition of intersegmental blood vessel formation in zebrafish embryos, as observed under a confocal microscope (Figure 6). In the control group, one embryo showed both

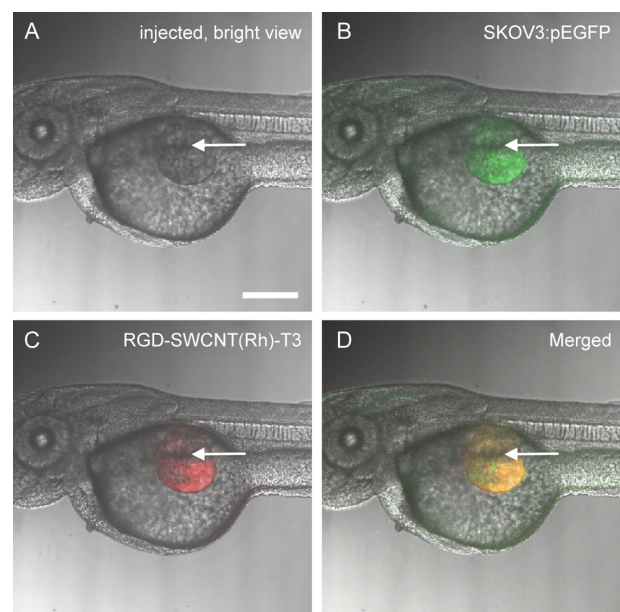


Figure 7 Tumor xenograft model in zebrafish embryos. Zebrafish embryos have been microinjected with fluorescently-labeled SKOV3:pEGFP mammalian cells suspended in Matrigel. The microinjection was conducted through the perivitelline space between the yolk and the periderm, close to the developing SIVs. The injection site is indicated by bright view in (A) using a white arrow, green fluorescence in (B) indicates presence of fluorescently-labeled SKOV3:pEGFP mammalian cells after injection, red fluorescence in (C) indicates presence of RGD-SWCNT(Rh)-thalidomide after injection, and (D) is (B) and (C) merged together. Scale bar: 150 μ m.

Abbreviations: RGD, cyclic arginine-glycine-aspartic peptide; SWCNT, single-walled carbon nanotubes; Rh, rhodamine; EGFP, enhanced green fluorescent protein; SIVs, subintestinal vessels.

absence and thinning of intersegmental blood vessels. Among the 20 thalidomide-SWCNT-treated embryos, 11 showed both absence and thinning of intersegmental blood vessels, three showed thinning of intersegmental blood vessels, and six did not show any effects. The intersegmental blood vessels were normally patterned in the treated embryos, and the absence or thinning of intersegmental blood vessels was randomly distributed (indicated by white arrows in Figure 6), showing depleted expression of the *fli1a* endothelial marker. Except for inhibition on intersegmental blood vessel formation, deleterious effects were not observed on the general morphology of embryonic structures by 48 hours following fertilization (data not shown). When assessed at 48 hours following fertilization, the treated embryos were both mobile and responsive to stimuli. These results confirm that thalidomide-SWCNT possess antiangiogenic activity against angiogenic vessel formation, and can be used for angiogenesis inhibition in zebrafish embryos.

Targeted antiangiogenesis therapy using RGD-SWCNT(Rh)-thalidomide

The tumor xenograft model in zebrafish embryos used in this study is illustrated in Figure 7. The mammalian SKOV3 cells

were transected with pEGFP, and stable SKOV3:pEGFP clones were resuspended in Matrigel and microinjected in the zebrafish embryos at 48 hours following fertilization (1000–2000 cells/embryo) through the perivitelline space between the yolk and the periderm (duct of Cuvier area), close to the developing subintestinal vessels (Figure 7A and B). Due to the immaturity of the immune system in zebrafish embryos until 48–72 hours following fertilization, no graft rejection occurred at this stage.²⁸ The nanoconjugates for antiangiogenesis, ie, RGD-SWCNT(Rh)-thalidomide, were simultaneously administrated at the same site (Figure 7C).

By imaging transgenic *fli1a:EGFP* zebrafish that contained fluorescently-labeled endothelial cells, tumor angiogenesis, including subintestinal vessel development, can be observed in transgenic zebrafish embryos under both fluorescent and confocal microscopy by checking the GFP signal. As shown in Figure 8, control embryos (Figure 8A) injected with Matrigel develop subintestinal vessels on the surface of the yolk in the shape of a basket. The use of proangiogenic tumor cell xenografts in zebrafish embryos allows continuous delivery of angiogenic factors produced by a limited number of tumor cells. The proangiogenic behavior of human HT1080 tumor cells is demonstrated in the xenografted zebrafish embryos.

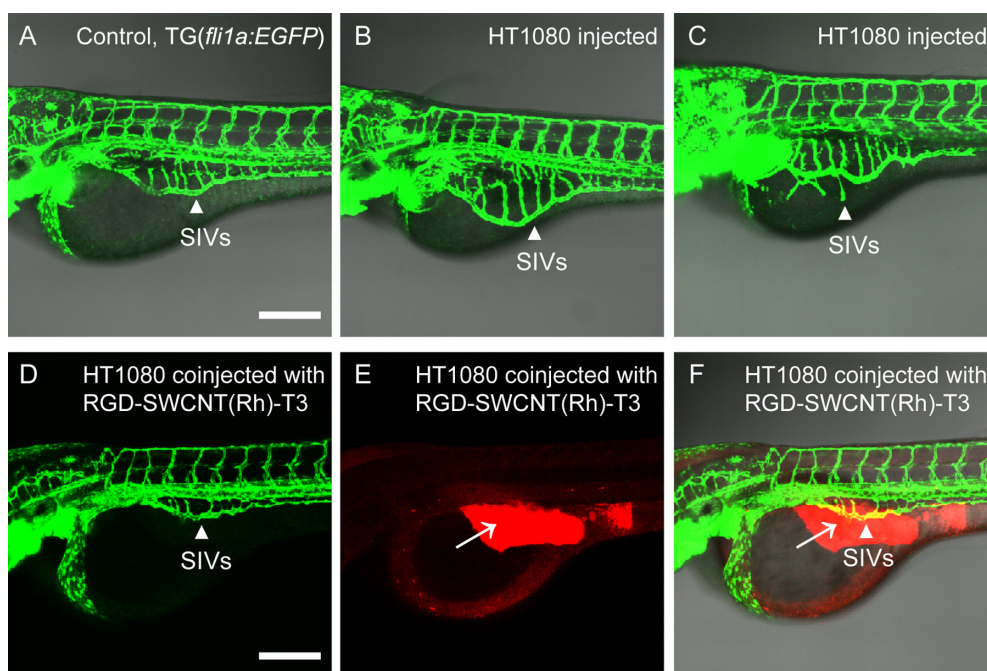


Figure 8 Blood vessels of transgenic *fli1a:EGFP* zebrafish embryos can be easily observed under the confocal microscope (A), and SIVs are marked by white arrows. Angiogenic responses (B and C) are triggered by tumor cell xenografts and targeted antiangiogenic therapy of RGD-SWCNT(Rh)-thalidomide (D, E and F) in transgenic *fli1a:EGFP* zebrafish embryos. Engraftment of human HT1080 fibrosarcoma cells, which secrete vascular endothelial growth factors, triggers ectopic angiogenesis of SIVs (B and C). Note morphological features of angiogenic response with engraftment of human HT1080 fibrosarcoma cells. When coinjected with RGD-SWCNT(Rh)-thalidomide (E), ectopic growth of angiogenesis of the SIV is obviously inhibited (D and F) in treated zebrafish embryos. White arrows (E and F) indicate presence of RGD-SWCNT(Rh)-thalidomide after injection. (F) is the merge of (D) and (E). Scale bar: 200 μ m.

Abbreviations: RGD, cyclic arginine-glycine-aspartic peptide; SWCNT, single-walled carbon nanotubes; Rh, rhodamine; EGFP, enhanced green fluorescent protein; SIVs, subintestinal vessels.

As compared with the control embryos (Figure 8A), those injected with HT1080 cells (Figure 8B and C) show increased ectopic subintestinal vessel angiogenesis. Xenograftment of HT1080 cells induced an increase in the size of the area encompassed by the entire subintestinal vessel basket, as shown in Figure 8B. In some cases, xenograftment with proangiogenic mammalian HT1080 tumor cells induced the appearance of long spikes that project from the subintestinal vessel basket (long arrows), as shown in Figure 8C. Integrin $\alpha_v\beta_3$ is highly expressed on activated endothelial cells, and the cyclic RGD peptide recognizes $\alpha_v\beta_3$ integrin receptors. Here, RGD-labeled nanoconjugates specifically targeted the angiogenesis site in the subintestinal vessel area, and the coated antiangiogenic drug, thalidomide, inhibited ectopic angiogenesis. As shown in Figure 8D and F, 1.6 ng of modified thalidomide (red signal in Figure 8E, with 4.8 ng of SWCNT and 0.6 ng RGD) had an obvious angiogenesis inhibition effect on loaded zebrafish embryos. Furthermore, existing normal blood vessels, such as the subintestinal vessels, were not affected by administration of the nanoconjugates. No deaths were observed during any of the treatments.

The extent of inhibition efficacy using RGD-SWCNT(Rh)-thalidomide varies in different embryos. Overall basket area and total vessel length within the subintestinal vessel basket area were quantified using the NIH Image program. As shown in Figure 9, in comparison with the control embryos, treatment with proangiogenic HT1080 tumor cells increased the subintestinal vessel growth by increasing both subintestinal vessel area and total subintestinal vessel length. Treatment with RGD-SWCNT(Rh)-thalidomide reduced ectopic subintestinal vessel growth, as shown in Figure 9, by reducing both subintestinal vessel area and total subintestinal vessel length. The inhibition efficacy of thalidomide-SWCNT(Rh)-RGD nanoconjugates was also affected by its loading site and distribution profile. When loading was limited to the xenograft site, ectopic angiogenesis of the subintestinal vessel was reduced (Figure 8D and E). When the distribution profile was expanded to whole embryos, including the whole yolk area and the circulation system, subintestinal vessel development was completely inhibited (data not shown).

Discussion

The potential for toxic effects of drugs and difficulty in limiting drug uptake are major considerations for most delivery systems. Administration by incubating zebrafish embryos in a drug solution is not able to control the drug uptake and thus the effect will be systemic, but not local. Administration by injection can reduce the drug amount and improve drug uptake in a

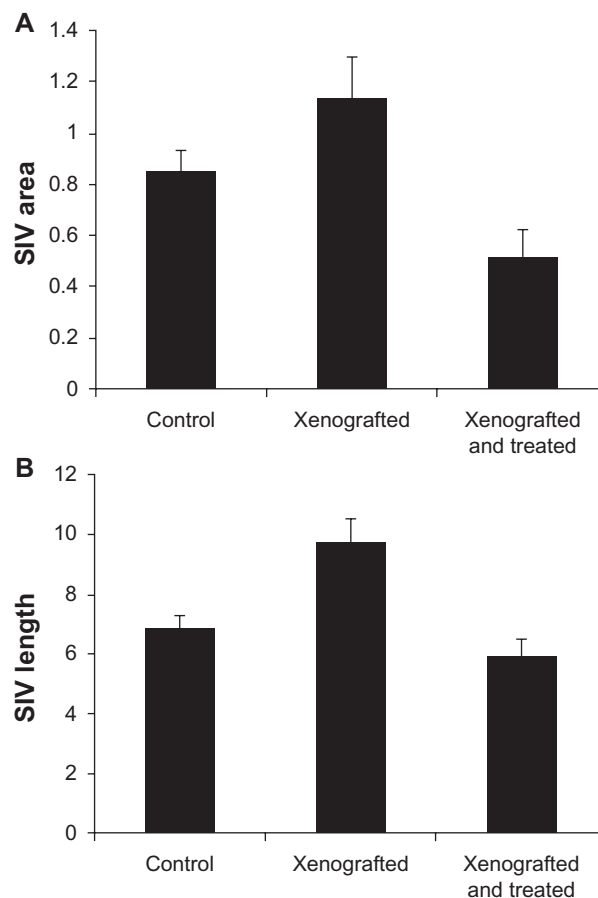


Figure 9 Total SIV length and area measurements in the zebrafish angiogenesis assay. The transgenic *flil1a:EGFP* zebrafish was used to study in vivo angiogenesis. By imaging live transgenic *flil1a:EGFP* zebrafish that contained fluorescently labeled endothelial cells at 72 hours following fertilization, the blood vessels are visualized under confocal microscopy. The total SIV vessel length and area is determined by using the NIH Image program. Each bar represents the mean \pm standard deviation ($n = 15$). The control group refers to embryos injected with Matrigel only, the xenografted group refers to embryos xenografted with proangiogenic mammalian tumor cells HT1080, and the xenografted and treated group refers to embryos xenografted with proangiogenic tumor cells together with antiangiogenic nanoconjugates RGD-SWCNT(Rh)-thalidomide.

Abbreviations: RGD, cyclic arginine-glycine-aspartic peptide; SWCNT, single-walled carbon nanotubes; Rh, rhodamine; EGFP, enhanced green fluorescent protein; SIV, subintestinal vessel.

desired location. However, administration by injection without targeting can potentially induce systemic toxic effects. Administering drugs by conjugation to a multimodal drug vector can combine the drugs together with the targeting molecules, thus improving drug uptake and minimizing side effects.

Functionalized carbon nanotubes are an emerging nanovector for the delivery of therapeutics, and functionalization strategies are a key step for the integration of carbon nanotubes into different systems for potential applications. Many functionalization strategies have been investigated for multimodal drug delivery. Previous studies have demonstrated that carbon nanotubes can be functionalized with two different molecules, ie, a drug and a fluorescent probe.²⁹

SWCNT have also been functionalized with both oligonucleotides and a folate moiety to achieve selective cancer cell destruction.⁸ Recently, the triple functionalization strategy of SWCNT with a drug, targeting moiety, and fluorescent marker has also been developed for targeted cancer therapy.³⁰ In this work, we present a method for triple functionalization of SWCNT with three moieties on the surface to achieve targeted delivery of small doses of antiangiogenic drugs to newly formed blood vessels, and we have further assessed its efficacy in transparent zebrafish embryos. This work presents a new functionalization approach to equip purified SWCNT with three different agents for targeted drug delivery. The present methodology allows for targeted delivery of an antiangiogenic drug to tumor sites and visualization of the distribution of SWCNT by confocal microscopy. It is interesting to note that all the molecules attached onto carbon nanotubes preserved their functions after the conjugation process. These findings indicate that carbon nanotubes, especially SWCNT, have considerable potential for improving drug delivery.

Acknowledgments

The work described in this paper was substantially supported by grants from the Research Grants Council of the Hong Kong Special Administrative Region to SHC and WTW (Project No. CityU 160107 and CityU 160108). YJG was supported by a postdoctoral fellowship Research Enhancement Scheme from the City University of Hong Kong. We also acknowledge the Zebrafish International Resource Center for providing us with the transgenic *fli1a:EGFP* zebrafish line.

Disclosure

The authors report no conflicts of interest in this work.

References

- Dickson PV, Nathwani AC, Davidoff AM. Delivery of antiangiogenic agents for cancer gene therapy. *Technol Cancer Res Treat*. 2005;4(4):331–341.
- Cai W, Chen X. Anti-angiogenic cancer therapy based on integrin α -v β 3 antagonism. *Anticancer Agents Med Chem*. 2006;6(5):407–428.
- Griffioen AW, Molema G. Angiogenesis: Potentials for pharmacologic intervention in the treatment of cancer, cardiovascular diseases, and chronic inflammation. *Pharmacol Rev*. 2000;52(2):237–268.
- Li ZB, Cai W, Cao Q, et al. (64)Cu-labeled tetrameric and octameric RGD peptides for small-animal PET of tumor α (v) β 3 integrin expression. *J Nucl Med*. 2007;48(7):1162–1171.
- Ke T, Jeong EK, Wang X, Feng Y, Parker DL, Lu ZR. RGD targeted poly(L-glutamic acid)-cystamine-(Gd-DO3A) conjugate for detecting angiogenesis biomarker α (v) β 3 integrin with MRT mapping. *Int J Nanomedicine*. 2007;2(2):191–199.
- Lacerda L, Bianco A, Prato M, Kostarelos K. Carbon nanotubes as nanomedicines: From toxicology to pharmacology. *Adv Drug Deliv Rev*. 2006;58(14):1460–1470.
- Pantarotto D, Briand JP, Prato M, Bianco A. Translocation of bioactive peptides across cell membranes by carbon nanotubes. *Chem Commun (Camb)*. 2004;1:16–17.
- Kam NW, O'Connell M, Wisdom JA, Dai H. Carbon nanotubes as multifunctional biological transporters and near-infrared agents for selective cancer cell destruction. *Proc Natl Acad Sci U S A*. 2005;102(33):11600–11605.
- Cheng JP, Chan CM, Veca LM, et al. Acute and long-term effects after single loading of functionalized multi-walled carbon nanotubes into zebrafish (*Danio rerio*). *Toxicol Appl Pharmacol*. 2009;235(2):216–225.
- Isogai S, Lawson ND, Torrealday S, Horiguchi M, Weinstein BM. Angiogenic network formation in the developing vertebrate trunk. *Development*. 2003;130(21):5281–5290.
- Childs S, Chen JN, Garrity DM, Fishman MC. Patterning of angiogenesis in the zebrafish embryo. *Development*. 2002;129(4):973–982.
- Serbedzija GN, Flynn E, Willett CE. Zebrafish angiogenesis: A new model for drug screening. *Angiogenesis*. 1999;3(4):353–359.
- Chan J, Bayliss PE, Wood JM, Roberts TM. Dissection of angiogenic signaling in zebrafish using a chemical genetic approach. *Cancer Cell*. 2002;1(3):257–267.
- Larson JD, Wadman SA, Chen E, et al. Expression of *VE-cadherin* in zebrafish embryos: A new tool to evaluate vascular development. *Dev Dyn*. 2004;231(1):204–213.
- Weinstein BM. Plumbing the mysteries of vascular development using the zebrafish. *Semin Cell Dev Biol*. 2002;13(6):515–522.
- Rajkumar SV, Witzig TE. A review of angiogenesis and antiangiogenic therapy with thalidomide in multiple myeloma. *Cancer Treat Rev*. 2000;26(5):351–362.
- Figg WD, Dahut W, Duray P, et al. A randomized phase II trial of thalidomide, an angiogenesis inhibitor, in patients with androgen-independent prostate cancer. *Clin Cancer Res*. 2001;7(7): 1888–1893.
- Lawson ND, Weinstein BM. In vivo imaging of embryonic vascular development using transgenic zebrafish. *Dev Biol*. 2002;248(2):307–318.
- Cheng SH, Wai AWK, So CH, Wu RSS. Cellular and molecular basis of cadmium-induced deformities in zebrafish embryos. *Environ Toxicol Chem*. 2000;19(12):3024–3031.
- Kimmel CB, Ballard WW, Kimmel SR, Ullmann B, Schilling TF. Stages of embryonic-development of the zebrafish. *Dev Dyn*. 1995;203(3):253–310.
- Nicoli S, Presta M. The zebrafish/tumor xenograft angiogenesis assay. *Nat Protoc*. 2007;2(11):2918–2923.
- Lin Y, Taylor S, Li HP, et al. Advances toward bioapplications of carbon nanotubes. *J Mater Chem*. 2004;14:527–541.
- Schellenberger EA, Sosnovik D, Weissleder R, Josephson L. Magneto/optical annexin V, a multimodal protein. *Bioconjug Chem*. 2004;15(5):1062–1067.
- Fang C, Bhattarai N, Sun C, Zhang M. Functionalized nanoparticles with long-term stability in biological media. *Small*. 2009;5(14):1637–1641.
- Niethammer P, Grabher C, Look AT, Mitchison TJ. A tissue-scale gradient of hydrogen peroxide mediates rapid wound detection in zebrafish. *Nature*. 2009;459(7249):996–999.
- Crivellato E, Ribatti D. Cross-link between inflammation and angiogenesis. In: Domenico Ribatti, editor. *Recent Advances in Angiogenesis and Antiangiogenesis*. Karachi, Pakistan: Bentham Science; 2009.
- Creamer D, Allen M, Sousa A, Poston R, Barker J. Altered vascular endothelium integrin expression in psoriasis. *Am J Pathol*. 1995; 147(6):1661–1667.
- Nicoli S, Ribatti D, Cotelli F, Presta M. Mammalian tumor xenografts induce neovascularization in zebrafish embryos. *Cancer Res*. 2007;67(7):2927–2931.
- Pastorin G, Wu W, Wieckowski S, et al. Double functionalization of carbon nanotubes for multimodal drug delivery. *Chem Commun (Camb)*. 2006;11:1182–1184.
- Heister E, Neves V, Tilmaciu C, et al. Triple functionalisation of single-walled carbon nanotubes with doxorubicin, a monoclonal antibody, and a fluorescent marker for targeted cancer therapy. *Carbon*. 2009;47(9):2152–2160.

Supplementary materials and methods

Preparation of thalidomide analogs 1–5

Thalidomide **1** 100 mg (0.387 mmol) dissolved in 30 mL of dry DMF were added to sodium hydride (60%, 25 mg, 0.625 mmol) and stirred for 30 minutes. 2-(Boc-amino) ethyl bromide (130 mg, 0.58 mmol) was then added into the solution. The mixture was stirred at room temperature for 12 hours. The resulting mixture was extracted with ethyl acetate (30 mL \times 3), the organic layer was washed with saturated NaCl and dried (anhydrous Na₂SO₄), the solvent was evaporated under reduced pressure to afford thalidomide **2**. ¹H NMR (CDCl₃, 300 MHz) δ 7.78–7.83 (m, 2H, ArH), 7.67–7.72 (m, 2H, ArH), 4.88–4.96 (m, 1H, CH), 3.92–3.95 (m, 2H, NCH₂CH₂NH), 3.24–3.29 (m, 2H, NCH₂CH₂NH), 1.36 [s, 9H, C(CH₃)₃]: An analytical sample was obtained by silica column chromatography eluted with CH₂Cl₂. Compound **2** was then treated by trifluoroacetic acid in dichloromethane (CH₂Cl₂) for 4 hours to remove protective BOC groups. The solvent was evaporated under reduced pressure to afford **3**. ¹H NMR (MeOD, 300 MHz) δ 7.85–7.93 (m, 4H, ArH), 5.18–5.25 (dd, J₁ = 5.70 Hz, J₂ = 12.75 Hz, 1H, CH), 4.10–4.15 (m, 2H, NCH₂CH₂NH), 3.12–3.17 (m, 2H, NCH₂CH₂NH). Then the compound **3** was conjugated with S-acetylthioglycolic acid N-hydroxysuccinimide ester for 2 hours to obtain compound **4** (MS-ESI m/z (relative intensity): 440.4 (100%), followed

by thiol deprotection using hydroxylamine under neutral conditions to yield the thiolated thalidomide **5** (MS-ESI m/z [relative intensity]: 375.4) (100%), denoted as thalidomide-SH.

Abbreviations: DMF, dimethylformamide; NMR, nuclear magnetic resonance; MS, mass spectroscopy; ESI, electro-spray ionization.

Synthesis of functionalized SWCNT

A Preparation of PEGylated single-walled carbon nanotubes (SWCNT)

2. Raw SWCNT were first oxidized to obtain oxidized SWCNT **1**. Raw SWCNT 50 mg were oxidized to yield a functionalized SWCNT **1** using 50 mL of concentrated HNO₃ by sonicating for 1 hour, followed by heating at 100°C for 24 hours. The reaction mixture diluted to 500 mL with water was filtered through a polycarbonate filter (Whatman, pore size 0.22 μ m). The product was then washed thoroughly by water until the pH reached neutral conditions and further oven dried at 100°C under vacuum for 4 hours (40 mg, 80%). The oxidized SWCNT were then conjugated with PEG to get PEGylated SWCNT **2**. A suspension of the oxidized and cut SWCNT (30 mg) in 0.1 M phosphate-buffered solution (pH = 7.4) were mixed with EDC 60 mg and PEG_{3500N} 50 mg and sonicated for 24 hours to afford PEGylated SWCNT **2**. The aqueous suspension was then centrifuged at 12,000 rpm for about 1 hour to remove any large unreacted SWCNT from

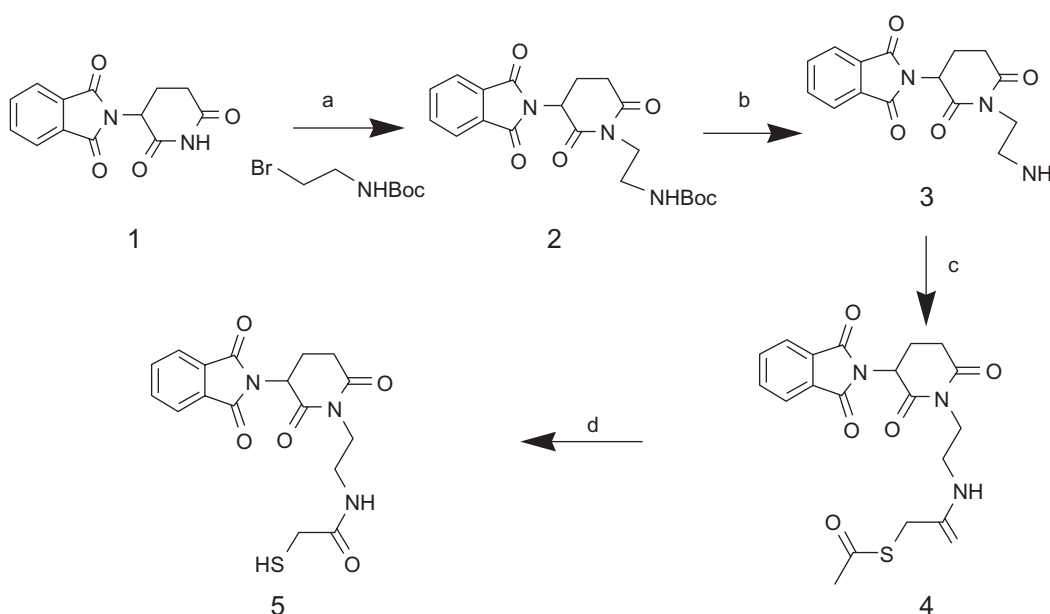


Figure S1 Synthesis of thalidomide analogs. Reagents and conditions are the following: (a) 2-(Boc-amino) ethyl bromide, trifluoroacetic acid, room temperature, 12 hours; (b) trifluoroacetic acid in CH₂Cl₂, 4 hours; (c) SATA, phosphate-buffered saline, 2 hours; (d) NH₂OH, ethylenediamine tetra-acetic acid, phosphate-buffered saline.

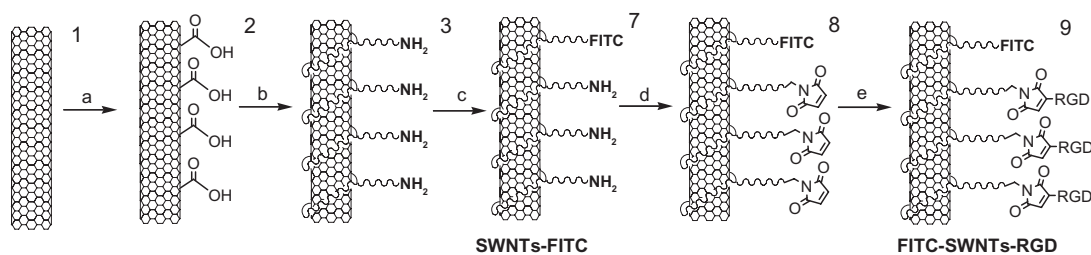


Figure S2 Synthesis route of SWCNT-FITC 7 and FITC-SWCNT-RGD 9 conjugates. (a) HNO_3 , 24 hours; (b) $\text{H}_2\text{N-PEG-NH}_2$, EDC, NHS, 0.1 M PBS, pH 7.4; (c) FITC, DMF, dark; (d) SMCC, DMSO; (e) RGD-SH, 0.1 M PBS.

Abbreviations: FITC, fluorescein isothiocyanate; RGD, cyclic arginine-glycine-aspartic peptide; SWCNT, single-walled carbon nanotubes; SMCC, succinimidyl 4-[N-maleimidomethyl]cyclohexane-1-carboxylate; DMSO, dimethyl sulfoxide; PBS, phosphate-buffered solution; EDC, 1-ethyl-3-(3-dimethylamino-propyl) carbodiimide; PEG, polyethylene glycol; DMF, dimethylformamide.

the solution. The resulting solution was then dialyzed against H_2O in a 12,000–14,000 molecular weight cutoff membrane (Spectro/Por dialysis tubing) for three days to yield PEGylated SWCNT-PEG- NH_2 . The resulting product was lyophilized overnight to give pure SWCNT-PEG- NH_2 .

Abbreviations: SWCNT, single-walled carbon nanotubes; EDC, 1-ethyl-3-(3-dimethylamino-propyl) carbodiimide; PEG, polyethylene glycol.

B Synthesis of Rh-SWCNT

The PEGylated SWCNT dissolved in 0.1 M phosphate-buffered solution was stirred overnight with NHS-Rh to afford Rh-SWCNT conjugates. The resulting solution was then dialyzed against H_2O in a 12,000–14,000 molecular weight cutoff membrane to remove excess Rh reagents.

Abbreviations: SWCNT, single-walled carbon nanotubes; Rh, rhodamine; PEG, polyethylene glycol; NHS, N-hydroxy succinimide.

C Preparation of Rh-SWCNT-SMCC, Rh-SWCNT-RGD and RGD-SWCNT(Rh)-thalidomide nanoconjugates

20 mg of SMCC in 2 mL of DMSO was added to a solution of Rh-SWCNT (5 mL) in 0.1 M phosphate-buffered solution (supplemented with 0.3 M NaCl, pH = 7.4). The mixture was allowed to react at room temperature for 2 hours, after which the conjugate was dialyzed against H_2O to remove excess SMCC linkers. For a preparation of RGD-SWCNT(Rh)-thalidomide conjugate, Rh-SWCNT-SMCC solution was concentrated by using a centrifugal device (10,000 or 30,000), and the volume was reduced to 5 mL. Then Rh-SWCNT-SMCC conjugate 4 was reacted overnight with RGD-SH and thalidomide-SH in the presence of 10 mM Tris(2-carboxyethyl)phosphine hydrochloride at pH 7.4. Excess RGD-SH and thalidomide-SH was removed by dialysis, in the same

manner as that described above, to yield RGD-SWCNT(Rh)-thalidomide and Rh-SWCNT-RGD conjugates.

The amount of RGD on SWCNT was estimated by bicinchoninic acid protein assay. We assumed that the concentration of SWCNT on Rh-SWCNT and RGD-SWCNT(Rh)-thalidomide are the same. The enzyme-linked immunosorbent assay at 470 nm was performed on RGD-SWCNT(Rh)-thalidomide, RGD (as a positive control), and SWCNT(Rh) + RGD (as a negative control) with various concentrations to establish calibration curves. Therefore, the loading of RGD on SWCNT was calculated from a calibration curve of Rh-SWCNT + RGD conjugates. The amount of RGD on SWCNT was 0.125 mg/mg. Ultraviolet-visible measurement was carried out using a spectrophotometer. Concentration of thalidomide loaded onto the SWCNT was measured by the absorbance peak at 299 nm (characteristic of thalidomide). We assumed that the concentration of SWCNT on Rh-SWCNT and RGD-SWCNT(Rh)-thalidomide are the same. The ultraviolet-visible measurement of Rh-SWCNT + RGD at various concentrations was performed to establish calibration curves. The concentration of thalidomide on SWCNT was estimated to be 0.334 mg/mg.

Abbreviations: RGD, cyclic arginine-glycine-aspartic peptide; SWCNT, single-walled carbon nanotubes; Rh, rhodamine; SMCC, succinimidyl 4-[N-maleimidomethyl]cyclohexane-1-carboxylate; DMSO, dimethyl sulfoxide.

D Synthesis of FITC-SWCNT and FITC-SWCNT-RGD (Scheme S2)

The PEGylated SWCNT in 10 mL of 0.1 M phosphate-buffered solution (pH 8.0) was added a solution of FITC in DMF (18 mg, 0.046 mmol). The mixture was then stirred overnight at room temperature. The resulting solution was then dialyzed against H_2O in a 12,000–14,000 molecular weight cutoff membrane to remove free FITC. Then, 20 mg

of SMCC in 2 mL of DMSO was added to a solution of SWCNT-FITC (5 mL) in 0.1 M phosphate-buffered solution (supplemented with 0.3 M NaCl, pH = 7.4). Excess SMCC was removed by dialysis to yield FITC-SWCNT-SMCC. RGD-SH was added into FITC-SWCNT-SMCC in 2 mL 0.1 M phosphate-buffered solution. The resulting suspension was stirred overnight at room temperature. Unreacted RGD-SH was removed by dialysis, in the same manner as that described above.

Abbreviations: FITC, fluorescein isothiocyanate; RGD, cyclic arginine-glycine-aspartic peptide; SWCNT, single-walled carbon nanotubes; Rh, rhodamine; SMCC, succinimidyl 4-[N-maleimidomethyl]cyclohexane-1-carboxylate; DMSO, dimethyl sulfoxide, DMF, dimethylformamide.

International Journal of Nanomedicine

Publish your work in this journal

The International Journal of Nanomedicine is an international, peer-reviewed journal focusing on the application of nanotechnology in diagnostics, therapeutics, and drug delivery systems throughout the biomedical field. This journal is indexed on PubMed Central, MedLine, CAS, SciSearch®, Current Contents®/Clinical Medicine,

Submit your manuscript here: <http://www.dovepress.com/international-journal-of-nanomedicine-journal>

Journal Citation Reports/Science Edition, EMBase, Scopus and the Elsevier Bibliographic databases. The manuscript management system is completely online and includes a very quick and fair peer-review system, which is all easy to use. Visit <http://www.dovepress.com/testimonials.php> to read real quotes from published authors.

Dovepress